International Journal of Engineering, Mathematical and Physical Sciences
ISSN: 2517-9934
Vol:6, No:3, 2012

Quantum computation using two component Bose-Einstein condensates

Tim Byrnes

Abstract—Quantum computation using qubits made of two component Bose-Einstein condensates (BECs) is analyzed. We construct a general framework for quantum algorithms to be executed using the collective states of the BECs. The use of BECs allows for an increase of energy scales via bosonic enhancement, resulting in two qubit gate operations that can be performed at a time reduced by a factor of N, where N is the number of bosons per qubit. We illustrate the scheme by an application to Deutsch's and Grover's algorithms, and discuss possible experimental implementations. Decoherence effects are analyzed under both general conditions and for the experimental implementation proposed.

Keywords—Quantum, computing, information, Bose-Einstein condensates, macroscopic.

I. Introduction

BOSE-EINSTEIN condensation first achieved in 1995 [1] has now been achieved in a wide variety of systems, ranging from ultracold atoms [2], exciton-polaritons [3], magnons [4], and photons [5]. For atomic Bose-Einstein condensates (BECs), atom chip technology has made possible the miniaturization of traps on the micrometer scale, allowing for the possibility of the individual formation and control of many BECs [6]. Exciton-polaritons in semiconductor microcavities of comparable dimensions provide similar possibilities of scaling up to many BECs on a single chip [3]. A natural application for such systems is quantum information processing, ranging from such tasks as quantum metrology [7], quantum simulation [8], and quantum computing.

In a recent set of experiments, two component BECs were realized on atom chips realizing full single qubit control on the Bloch sphere and spin squeezing [10], [9], [11]. Currently, the primary application for such two component BECs is for quantum metrology and chip based clocks. In this paper we discuss its applications towards quantum computation. Although BECs have been considered for quantum computation in the past [12], the results have shown to be generally been unfavorable for these purposes due to enhanced decoherence effects due to the large number of bosons N in the BEC. In this work we consider a different encoding of the quantum information, which to a large extent mitigates this problem. We develop the framework for quantum computation using this encoding, illustrated with several quantum algorithms.

One of the key features that we take advantage of is the bosonic enhancement effect for many bosons. As is well known from optical manipulation of atomic states, matrix elements involving boson operators are enhanced by a factor of $\sqrt{N}$, where N is the number of bosons. For example, the Rabi frequency of an optically controlled two level system scales as the square root of the intensity of the laser field. In the case of BECs, the large number of bosons forming the BEC results in an enhancement of the energy scale of the control Hamiltonians. This allows for gate times to be decreased in time by a factor of N, which is typically of the order of $\sim 10^3$ for atom chip BECs. Combining this with optical manipulation (which provide a bosonic enhancement of their own), this allows for a method for fast manipulations of the quantum state within a limited decoherence time. Similar approaches for semiconductor quantum dots have resulted in the demonstration of ultrafast coherent manipulations of single qubit states [13], [14], [15].

T. Byrnes is at the National Institute of Informatics, Tokyo, Japan e-mail: tbyrnes@nii.ac.jp (see http://www.nii.ac.jp/en/faculty/informatics/BYRNES-Tim).

II. Single qubit encoding

Consider a BEC consisting of bosons with two independent degrees of freedom, such as two hyperfine levels in an atomic BEC or spin polarization states of exciton-polaritons [7], [3]. Denote the bosonic annihilation operators of the two states as a and b, obeying commutation relations $[a, a^\dagger] = [b, b^\dagger] = 1$ [16]. We encode a standard qubit state $\alpha|0\rangle + \beta|1\rangle$ in the BEC in the state

$$|\alpha, \beta\rangle\rangle \equiv \frac{1}{\sqrt{N!}} \left(\alpha a^\dagger + \beta b^\dagger\right)^N |0\rangle, \tag{1}$$

where α and β are arbitrary complex numbers satisfying $|\alpha|^2 + |\beta|^2 = 1$ (double brackets are used to denote the bosonic qubit states). For simplicity let us first consider the boson number $N = a^\dagger a + b^\dagger b$ to be a conserved number. Each qubit state is therefore encoded by N bosonic particles with a collective Hilbert space dimension of $N + 1$.

The state (1) can be visualized by a vector on the Bloch sphere with an angular representation $\alpha = \cos(\theta/2), \beta = \sin(\theta/2)e^{i\phi}$. The state $|\alpha, \beta\rangle\rangle$ can be manipulated using Schwinger boson (Stokes operators) operators $S^x = a^\dagger b + b^\dagger a$, $S^y = -ia^\dagger b + ib^\dagger a$, $S^z = a^\dagger a - b^\dagger b$, which satisfy the usual spin commutation relations $[S^i, S^j] = 2i\epsilon_{ijk}S^k$, where ϵ_{ijk} is the Levi-Civita antisymmetric tensor. In the spin language, (1) forms a spin-$N/2$ representation of the SU(2) group (we omit the factor of 2 in our spin definition for convenience). Single qubit rotations can be performed in a completely analogous fashion to regular qubits. For example, rotations around the z-axis of the Bloch sphere can be performed by an evolution

$$\begin{aligned} e^{-i\Omega S^z t}|\alpha, \beta\rangle\rangle &= \frac{1}{\sqrt{N!}} \sum_{k=0}^{N} \binom{N}{k} (\alpha a^\dagger e^{-i\Omega t})^k (\beta b^\dagger e^{i\Omega t})^{N-k} |0\rangle \\ &= |\alpha e^{-i\Omega t}, \beta e^{i\Omega t}\rangle\rangle. \end{aligned} \tag{2}$$

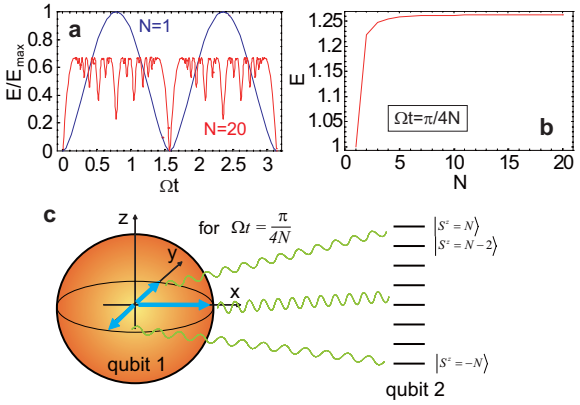

Fig. 1. **a** The entanglement normalized to the maximum entanglement ($E_{\max} = \log_2(N+1)$) between two bosonic qubits for the particle numbers as shown. **b** Entanglement at a time $\Omega t = \pi/4N$ for various boson numbers N. **c** A schematic representation of the entangled state (10).

Similar rotations may be performed around any axis by an application of

$$H_1 = \hbar\Omega \boldsymbol{n}\cdot\boldsymbol{S} = \hbar\Omega(n_x S^x + n_y S^y + n_z S^z) \tag{3}$$

where $\boldsymbol{n} = (n_x, n_y, n_z)$ is a unit vector. Expectation values of the spin are identical to that of a single spin (up to a factor of N), taking values

$$\begin{aligned}\langle S^x\rangle &= N(\alpha^*\beta + \alpha\beta^*)\\ \langle S^y\rangle &= N(-i\alpha^*\beta + i\alpha\beta^*)\\ \langle S^z\rangle &= N(|\alpha|^2 - |\beta|^2).\end{aligned} \tag{4}$$

The variance of the spins however diminish relative to the maximum amplitudes

$$\frac{\langle (S^z)^2\rangle - \langle S^z\rangle^2}{N^2} = \frac{4|\alpha\beta|^2}{N} \tag{5}$$

in accordance to widespread notion that for $N\to\infty$ the spins approach classical variables. We shall however see in the following section that despite the classical appearance of such a state, such a many boson state can exhibit quantum properties such as entanglement.

We note that collective state encodings have been proposed previously in works such as Refs. [18], [19], [17], where a large number of particles is used to encode a two level system. A key difference between the encoding in these works and (1) is that the full $N+1$ Hilbert space is used here to encode the two level system. The quantum state of a single qubit in (1) can be considered to be "duplicated" over N bosons, which are all in the same state. In previous works particular collective states are assigned to be the logical states. Thus although many physical particles encode the quantum state, the Hilbert space mapping is one-to-one. In this sense, the encoding presented here has similarities with quantum error correcting codes where an expanded Hilbert space is used to encode quantum states [20].

III. Two Qubit Entanglement

Two qubit gates can be formed by any product of the Schwinger boson operators of the form

$$H_2 = \sum_{i,j=x,y,z} \hbar\Omega_{ij} S_1^i S_2^j \tag{6}$$

where Ω_{ij} are real symmetric parameters. The combination of H_1 and H_2 may be combined to form an arbitrary Hamiltonian involving spin operators according to universality arguments [21]. By successive commutations an arbitrary product of spin Hamiltonians

$$H \propto \prod_{n=1}^{M} (S_n^j)^{m(n)} \tag{7}$$

may be produced, where M is the total number of qubits, $j = x, y, z$, and $m(n) = 0, 1$. Although in general higher order operators may be constructed (e.g. $m(n)\geq 2$), our aim here is to simulate the standard qubit system using the BEC qubits. Since for Pauli operators $(\sigma^j)^2 = 1$, such higher order operators are unnecessary for our purposes.

A key difference between Pauli operators and the Schwinger boson operators are that $\sigma^j \sim O(1)$, whereas $S^j \sim O(N)$. This makes the two qubit interaction $H_2 \sim O(N^2)$. The consequence of the boosted energy scale of the interaction can be observed by examining explicitly the state evolution of two qubits. For simplicity, let us consider henceforth consider the interaction Hamiltonian

$$H_2 = \hbar\Omega S_1^z S_2^z. \tag{8}$$

This may be done without any loss of generality since (7) can be converted to (8) by universality arguments. As a simple illustration, let us perform the analogue of the maximally entangling operation

$$e^{-i\sigma_1^z\sigma_2^z\frac{\pi}{4}}(|\uparrow\rangle + |\downarrow\rangle)(|\uparrow\rangle + |\downarrow\rangle) = |+y\rangle|\uparrow\rangle + |-y\rangle|\downarrow\rangle, \tag{9}$$

where $|\pm y\rangle = e^{\mp i\frac{\pi}{4}}|\uparrow\rangle + e^{\pm i\frac{\pi}{4}}|\downarrow\rangle$. Starting from two unentangled qubits, we may apply H_2 to obtain

$$\begin{aligned}&e^{-i\Omega S_1^z S_2^z t}|\frac{1}{\sqrt{2}},\frac{1}{\sqrt{2}}\rangle\rangle|\frac{1}{\sqrt{2}},\frac{1}{\sqrt{2}}\rangle\rangle\\ &= \frac{1}{\sqrt{2^N}}\sum_{k_2}\sqrt{\binom{N}{k_2}}|\frac{e^{i(N-2k_2)\Omega t}}{\sqrt{2}},\frac{e^{-i(N-2k_2)\Omega t}}{\sqrt{2}}\rangle\rangle|k_2\rangle,\end{aligned} \tag{10}$$

where we have introduced normalized eigenstates of the S^z operator $|k\rangle \equiv \frac{(a^\dagger)^k(b^\dagger)^{N-k}}{\sqrt{k!(N-k)!}}|0\rangle$. For gate times equal to $\Omega t = \pi/4N$ we obtain the analogous state to (9). For example, the maximum z eigenstates $|k_2 = 0, N\rangle$ on qubit 2 are entangled with the states $|\pm y\rangle\rangle \equiv |\frac{e^{\pm i\pi/4}}{\sqrt{2}},\frac{e^{\mp i\pi/4}}{\sqrt{2}}\rangle\rangle$, which is the analogue of a Bell state for the bosonic qubits. A visualization of the state (10) is shown in Figure 1c. For each z-eigenstate on qubit 2, there is a state $|\frac{e^{i(N-2k_2)\pi/4N}}{\sqrt{2}},\frac{e^{-i(N-2k_2)\pi/4N}}{\sqrt{2}}\rangle\rangle$ on qubit 1 represented on the Bloch sphere entangled with it. The type of entangled state is a continuous version of the original qubit sequence (9), and has similarities to continuous variable

formulations of quantum computing [22], although the class of states that are used here are quite different.

We note here that the analogue of the CNOT gate can be produced by further evolving (10) with the Hamiltonian $H_2' = \hbar\Omega(NS_1^z - NS_2^z + N^2)$ for a time $\Omega t = \pi/4N$. For example, for initial states where qubit 1 (2) is in an x- (z-) eigenstate, we obtain

$$U_{\text{CNOT}}|\frac{1}{\sqrt{2}},\pm\frac{1}{\sqrt{2}}\rangle\rangle|0,1\rangle\rangle = |\frac{1}{\sqrt{2}},\pm\frac{1}{\sqrt{2}}\rangle\rangle|0,1\rangle\rangle$$
$$U_{\text{CNOT}}|\frac{1}{\sqrt{2}},\pm\frac{1}{\sqrt{2}}\rangle\rangle|1,0\rangle\rangle = |\frac{1}{\sqrt{2}},\mp\frac{1}{\sqrt{2}}\rangle\rangle|1,0\rangle\rangle, \qquad (11)$$

which is exactly the same result as for standard qubits, where $U_{\text{CNOT}} = e^{-i(H_2+H_2')\pi/4N\Omega}$. However, due to the property of BEC qubits that $|\frac{1}{\sqrt{2}},\frac{1}{\sqrt{2}}\rangle\rangle \neq [|1,0\rangle\rangle + |0,1\rangle\rangle]/\sqrt{2}$, we cannot simply superpose (11) to obtain the intermediate cases. Nevertheless, the evolved states have similar properties to the standard qubit case. For example,

$$U_{\text{CNOT}}|\frac{1}{\sqrt{2}},\frac{1}{\sqrt{2}}\rangle\rangle|\frac{1}{\sqrt{2}},\frac{1}{\sqrt{2}}\rangle\rangle =$$
$$\frac{1}{\sqrt{2^N}}\sum_{k_2}\sqrt{\binom{N}{k_2}}|\frac{e^{-i\pi k_2/N}}{\sqrt{2}},\frac{1}{\sqrt{2}}\rangle\rangle|k_2\rangle. \qquad (12)$$

The correspondence to a CNOT operation may be seen by looking at the extremal states $|k_2 = 0, N\rangle$ states on qubit 2. These states are entangled with the states $|\pm\frac{1}{\sqrt{2}},\frac{1}{\sqrt{2}}\rangle\rangle$ on qubit 1 which is the same result as for a standard qubit CNOT operation with the target qubit in the x-basis for qubit 1. As was the case for Figure 1c, there are a pseudo-continuum of intermediate states between these extremal states. For BEC qubits it is the collective set of all the intermediate states that constitute the entanglement between the two qubits.

The effect of the boosted energy scale of (8) is that a gate time of $\Omega t = \pi/4N$ was required to produce this entangled state, in comparison to the standard qubit case of $\Omega t = \pi/4$. The origin of the reduced gate time is due to the bosonic enhancement of the interaction Hamiltonian, originating from the boosted energy scale via bosonic enhancement of many particles occupying the same quantum state in the BEC. An example of the speedup for the case of atom chips will be given in the section relating to the experimental implementation.

Despite the widespread belief that for $N \to \infty$ the spins approach classical variables according to (5), the entangling operation (10) generates genuine entanglement between the bosonic qubits. As a measure of the entanglement, we plot the von Neumann entropy $E = -\text{Tr}(\rho_1 \log_2 \rho_1)$ [20] in Figure 1a. For the standard qubit case ($N = 1$), the entropy reaches its maximal value at $\Omega t = \pi/4$ in accordance with (9). For the bosonic qubit case there is an initial sharp rise, corresponding to the improvement in speed of the entangling operation, but later saturates to a non-maximal value due to the presence of the binomial factors in (10) biasing the states towards zero spin values. We show in the Appendix that this saturating value approaches $\lim_{N\to\infty} E/E_{\max} \approx 1/2$, showing that macroscopic entanglement can indeed survive even in the "classical" limit of $N \to \infty$. In Figure 1b we show the amount of entanglement present at times $\Omega t = \pi/4N$. We see

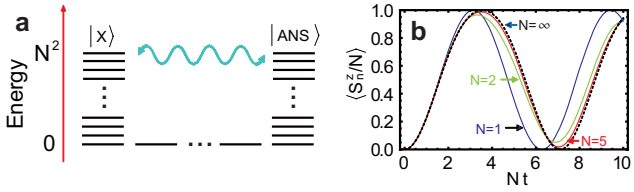

Fig. 2. **a** Schematic energy level structure of the Grover Hamiltonian. Rabi oscillations take place between the initial x-eigenstate $|X\rangle$ and the solution state $|ANS\rangle$. **b** Rabi oscillations executed by the Grover Hamiltonian for $M = 2$ for various boson numbers as shown. The dotted line shows the mean field result corresponding to the $N \to \infty$ limit.

that at such times there is approximately the same amount of entanglement as for the $N = 1$ case as for large N, confirming that the $e^{-iS_1^z S_2^z \pi/4N}$ gate gives the bosonic analogy to the operation (9).

IV. Quantum Algorithms

Given a qubit algorithm intended for standard two-level qubits, how does this translate in the bosonic system? For many applications, the procedure amounts to: (i) finding the sequence of Hamiltonians required for the algorithm, (ii) making the replacement $\sigma_n^j \to NS_n^j$, $\sigma_n^i\sigma_m^j \to S_n^iS_m^j$, (iii) Evolving the same sequence of Hamiltonians for a reduced time $t \to t/N$. This approach is reasonable from the point of view that we are performing the same algorithm except that a higher representation of SU(2) is being used. Let us illustrate this procedure with two well-known quantum algorithms with speedups over classical algorithms.

A. Deutsch's algorithm

We reformulate the standard qubit version ($N = 1$) of the algorithm in the following form convenient for our purposes [20]. The oracle performing the function $|x\rangle|y\rangle \to |x\rangle|f(x) \oplus y\rangle$ is assumed to be one of the four Hamiltonians $H_D = \{0, 2\sigma_2^z, \sigma_1^z\sigma_2^z + \sigma_2^z - 1, -\sigma_1^z\sigma_2^z + \sigma_2^z - 1\}$ and evolved for a time $t = \pi/4$, which correspond to the functions $f(x) = \{(0,0),(1,1),(0,1),(1,0)\}$ respectively. The initial state is assumed to be the state $(\uparrow + \downarrow)\uparrow$, and a measurement of qubit 1 in the x-basis distinguishes between constant and balanced functions via the results $(\uparrow + \downarrow)$ and $(\uparrow - \downarrow)$ respectively.

This can be translated into the corresponding algorithm for bosonic qubits according to the following procedure. The oracle is assumed to be one of the following Hamiltonians $H_D = \{0, 2NS_2^z, S_1^zS_2^z + NS_2^z - N^2, -S_1^zS_2^z + NS_2^z - N^2\}$, and we prepare the initial state as $|\frac{1}{\sqrt{2}},\frac{1}{\sqrt{2}}\rangle\rangle|1,0\rangle\rangle$. After evolving the Hamiltonians for a time $t = \pi/4N$, we obtain (up to an overall phase)

$$e^{-iH_D\pi/4N}|\frac{1}{\sqrt{2}},\frac{1}{\sqrt{2}}\rangle\rangle|1,0\rangle\rangle = |\frac{1}{\sqrt{2}},\pm\frac{1}{\sqrt{2}}\rangle\rangle|1,0\rangle\rangle, \qquad (13)$$

where $+$ is obtained for the constant cases and $-$ for the balanced cases. A measurement of qubit 1 distinguishes the constant and balanced cases with one evaluation of the oracle.

B. Grover's algorithm

We use the continuous time formulation of the Grover search algorithm (see sec. 6.2 of Ref. [20]). For the standard qubit case ($N = 1$), a Hamiltonian $H_G = |X\rangle\langle X| + |ANS\rangle\langle ANS|$ is applied to an initial state $|X\rangle$. Here, $|X\rangle$ is the $\sigma_n^x = 1$ eigenstate of all the qubits and $|ANS\rangle$ is the solution state. Under this Hamiltonian evolution, the system executes Rabi oscillations between $|X\rangle$ and $|ANS\rangle$ with a period of $t = \pi\sqrt{2^M}$ where M is the number of qubits.

The bosonic version of the Hamiltonian can be constructed by mapping the projection operators according to $|j\rangle\langle j| = (1 + \sigma_n^j)/2 \to (1 + S_n^j/N)/2$, where $j = x, z$. The bosonic qubits are prepared in the state $|X\rangle = \prod_{n=1}^{M} |\frac{1}{\sqrt{2}}, \frac{1}{\sqrt{2}}\rangle\rangle_n$ and evolved in time by applying H. The system then executes Rabi oscillations between the initial state $|X\rangle$ and the solution state $|ANS\rangle$. The time required for a half period of the oscillation is found to be $t \sim \sqrt{2^M}/N$ (see Appendix), which has the same square root scaling with the number of sites, but with a further speedup of N, resulting from the fast gates made possible by the use of bosonic qubits. A numerical calculation for a simple two site case is shown in Figure 2b, which clearly shows the factor of N improvement in speed of the Grover algorithm.

V. Example experimental implementation

The above framework may be applied in general to a variety of different systems, such as atomic or exciton-polariton BECs as previously discussed. For concreteness, in this section we discuss the specific configuration of using BECs on atom chips, following the experimental configuration given in Refs. [11], [10], [9]. In these works, the $|F = 1, m_F = -1\rangle$ and $|F = 2, m_F = 1\rangle$ hyperfine levels of the $5S_{1/2}$ ground state of ^{87}Rb are used as the qubit states. In terms of Figure 3, we make the association for the operator $a^\dagger$ ($b^\dagger$) as creating an atom in the state $|F = 1, m_F = -1\rangle$ ($|F = 2, m_F = 1\rangle$). Since the BEC contains a large number of atoms, there can be more than one atom present in a particular level, as illustrated in Figure 3. Level "c" in Figure 3 corresponds to a suitable higher energy level satisfying optical selection rules determined by the polarization of the laser fields. Taking the $a \leftrightarrow c$ transitions to be σ^+ circularly polarized light, we make the association that the $c^\dagger$ operator creates an atom in the state $|F' = 2, m'_F = 0\rangle$ of the $5P_{3/2}$ state. The $b \leftrightarrow c$ transitions are then required to be σ^- polarized light, which connect $|F' = 2, m'_F = 0\rangle \leftrightarrow |F = 2, m_F = 1\rangle$.

Single qubit rotations may be performed according to existing methods using microwave pulses as discussed in Refs. [11], [10]. Here we propose an alternative method for single qubit rotations which naturally fits into the scheme for two qubit rotations (discussed below). Using detuned pulses we may connect levels a and b via an adiabatic passage using the two transitions shown in Figure 3. These are

$$H_1 = \Delta c^\dagger c + g(a^\dagger c + c^\dagger a) + g(b^\dagger c + c^\dagger b) \qquad (14)$$

Here $c^\dagger$ is a creation operator for a boson in level c and Δ is the detuning between the laser pulse and the transition energy. Assuming that $\Delta \gg g$, the effective coupling between levels a and b is then

$$H_1^{\text{eff}} = \hbar\Omega_1^{\text{eff}}(a^\dagger b + b^\dagger a) = \hbar\Omega_1^{\text{eff}} S^x \qquad (15)$$

where

$$\hbar\Omega_1^{\text{eff}} = \frac{g^2}{\Delta}. \qquad (16)$$

S^z rotations are performed by exploiting the natural energy difference between the $F = 1$ and $F = 2$ levels $\Omega_z/2\pi \sim 6.8$GHz, which allows for full control of the single qubit state on the Bloch sphere.

Two qubit gates may be implemented by using a quantum bus [24], which is implemented by connecting two BEC qubits via cavity QED, as shown in Figure 3. Recent experimental advances have allowed for the possibility of incorporating cavity QED with atom chips [25], [27]. We closely follow the methods in Ref. [28] and generalize to the bosonic case. In order to perform the entangling operation (18), the two BECs corresponding to the two qubits are placed within the cavity, with a resonant frequency detuned off the $b \leftrightarrow c$ transition as for the single qubit case. Due to the large detuning, without the presence of the second transition $a \leftrightarrow c$ (implemented by separate lasers), no population transfer between levels b and c take place. The two qubit gate can be turned on and off on demand by the application of the laser connecting levels a and c. This allows for an adiabatic passage between levels a and b of the form of the entangling gate as given in (18). To model such a system, consider an interaction Hamiltonian

$$H_2 = \frac{\hbar\omega_0}{2} \sum_{n=1,2} F_n^z + \hbar\omega p^\dagger p + G \sum_{n=1,2} \left[F_n^- p^\dagger + F_n^+ p\right], \qquad (17)$$

where $F^z = c^\dagger c - b^\dagger b$, $F^+ = c^\dagger b$, ω_0 is the transition frequency, and p is the photon annihilation operator. Assuming a large detuning $\Delta = \hbar\omega_0 - \hbar\omega \gg G$, we may adiabatically eliminate the photons from the bus by assuming $p^\dagger p = 0$ and we obtain an effective Hamiltonian $H_{\text{bus}} \approx \frac{G^2}{\Delta}\left(F_1^+ F_2^- + F_1^- F_2^+\right)$. Now consider a further detuned single qubit transition according to $H_{ac} = g\sum_{n=1,2}\left[c_n^\dagger a_n + \text{H.c}\right]$. After adiabatic elimination of level c by assuming $c_n^\dagger c_n = 0$, we obtain

$$H_2^{\text{eff}} \approx \hbar\Omega_2^{\text{eff}}(S_1^+ + S_2^+)(S_1^- + S_2^-) + \text{H.c.}. \qquad (18)$$

where

$$\hbar\Omega_2^{\text{eff}} = \frac{G^2 g^2}{\Delta^3}. \qquad (19)$$

The energy scale of the interaction term is then proportional to N^2 as claimed previously. Although this interaction involves undesired single qubit interaction terms $S^+S^- + S^-S^+ = -(S^z)^2/2 + \text{const.}$, these may be eliminated and converted to the form $\propto S_1^z S_2^z$ by combining with single qubit gates using universality arguments [21].

Initialization and readout can be performed using similar techniques to that already established in Refs. [10], [9], [11]. In short, initialization is performed in the preparation of the BEC state, which put the qubits in the $|1, 0\rangle\rangle$ state. Readout

is performed in the z-basis by absorption imaging following a time-of-flight sequence. We note that for our scheme single atom resolution is not necessary in the readout process since the each qubit is encoded as the collective total spin of the BEC. For example, in Deutsch's algorithm the final readout is achieved by a measurement of $\langle S_1^x \rangle$ which is a collective property of the BEC qubit.

VI. Decoherence for State Storage

We now consider decoherence effects due to the use of BEC qubits. Special emphasis will be made on the scaling properties of the decoherence with N, which is typically a large number in our case. Here we consider the case when a quantum state is stored in the system of qubits and no gates are applied, i.e. when the BEC qubits are used to simply store a state. The main channels of decoherence in this case are dephasing and particle loss. Considering dephasing first, we model this via the master equation

$$\frac{d\rho}{dt} = -\frac{\Gamma_z}{2}\sum_{n=1}^{M}[(S_n^z)^2\rho - 2S_n^z\rho S_n^z + \rho(S_n^z)^2], \qquad (20)$$

where Γ_z is the dephasing rate. For a standard qubit register, the information in a general quantum state can be reconstructed by $4^M - 1$ expectation values of $(I_1, S_1^x, S_1^y, S_1^z) \otimes (I_2, S_2^x, S_2^y, S_2^z) \cdots \otimes (I_M, S_M^x, S_M^y, S_M^z)$ [23]. For the bosonic system, there are in general higher order correlations involving powers of operators beyond order one, but these are unnecessary for our purposes as previously discussed.

Examining the dephasing of the general correlation $\langle \prod_n S_n^{j(n)} \rangle$ where $j(n) = I, x, y, z$, we obtain the evolution equation $d\langle \prod_n S_n^{j(n)} \rangle / dt = -2\Gamma_z K_z \langle \prod_n S_n^{j(n)} \rangle$, which can be solved to give

$$\langle \prod_n S_n^{j(n)} \rangle \propto \exp[-2\Gamma_z K_z t]. \qquad (21)$$

Here K_z is the number of non-commuting $S_n^{j(n)}$ operators with S_n^z (i.e. $j(n) = x, y$), which is independent of N and is at most equal to M. The crucial aspect to note here is that the above equation does not have any N dependence. In fact the equation is identical to that for the standard qubit case ($N = 1$). Physically this difference is due to the statistical independence of the dephasing processes among the bosons.

For particle loss, we consider the Hamiltonian

$$\frac{d\rho}{dt} = -\frac{\Gamma_l}{2}\sum_{n=1}^{M}[a_n^\dagger a_n \rho - 2a_n \rho a_n^\dagger + \rho a_n^\dagger a_n + b_n^\dagger b_n \rho - 2b_n \rho b_n^\dagger + \rho b_n^\dagger b_n], \qquad (22)$$

where Γ_l is the particle loss rate. We find the similar result

$$\langle \prod_n S_n^{j(n)} \rangle \propto \exp[-\Gamma_l K_l t], \qquad (23)$$

where K_l is the number of $S_n^{j(n)}$ operators that are not the identity (i.e. $j(n) = x, y, z$), which is again independent of N and is at most equal to M. The general results of (21) and (23) show that *decoherence is not enhanced by the use of BEC qubits when they are used to store a quantum state*. For an implementation using atom chip BECs, the dephasing time $1/\Gamma_z$ has been estimated to be on the order of seconds [11], a comparable time with other systems proposed for quantum computation [29].

The origin of this behavior is that powers of the spin operators beyond one (e.g. $(S_n^x)^2$) are not used to encode any quantum information in our scheme. An extreme case that would be highly susceptible to decoherence would be the use of Schrodinger cat states such as $\alpha|1,0\rangle\rangle + \beta|0,1\rangle\rangle$ to encode quantum information [12]. Such states are highly vulnerable to decoherence, due to the high order spin correlations $\langle (S_n^x)^N \rangle - \langle S_n^x \rangle^N$ present for such a state.

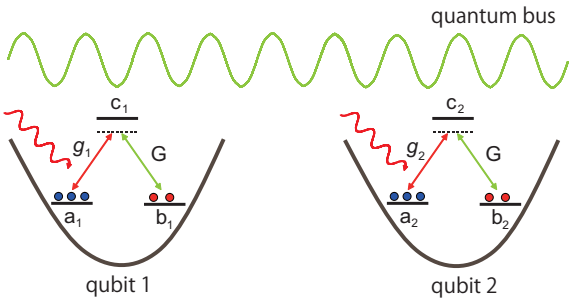

Fig. 3. Two bosonic qubits mediated by a quantum bus. The quantum bus couples transitions between levels b and c with energy G. Individual pulses coupling levels a and c with energy g create an adiabatic passage between levels a and b.

VII. Conclusion

We have found that two component BECs can form viable qubits that may be used for quantum computing. The theory is conceptually similar to the theory of continuous variables quantum information processing [22], where a large Hilbert space is used to encode qubit information. A mapping procedure for converting standard qubit quantum algorithms to the BEC qubit case was discussed and applied to Deutsch's and Grover's algorithms. The speed of such algorithms can be increased in speed by a factor of N, owing to the fast two qubit gates which arise due to the bosonic enhancement factor of the large number of bosons used. Importantly, decoherence effects due to the large number of bosons are not enhanced in these algorithms. A specific implementation using atom chips were discussed, together with expected decoherence effects associated with this implementation. Perhaps the most interesting result of this paper is that despite the "classical" $N \to \infty$ limit, entanglement can exist in the system when two qubit gates of the form $S_1^i S_2^j$ are applied. Although quantum fluctuations for variables such as S^i/N indeed do diminish in the limit $N \to \infty$, fluctuations for $\langle (S^i)^2 \rangle - \langle S^i \rangle^2 \sim O(\sqrt{N})$, thus should remain even for large BEC systems. This said, large amounts of entanglement between such BECs may in practice be difficult to observe for the same reason that Schrodinger cat states are difficult to observe, due to enhanced decoherence rates of such states. One aspect which we have not discussed is the bosonic mapping procedure for applications that use non-unitary operations such as measurements as part of the

algorithm, such as quantum teleportation. We leave such topics as future work.

ACKNOWLEDGMENT

This work is supported by Navy/SPAWAR Grant N66001-09-1-2024.

REFERENCES

[1] M. H. Anderson *et al.*, Science **269**, 198 (1995).
[2] J. R. Anglin and W. Ketterle, Nature **416**, 211 (2002).
[3] H. Deng, H. Haug, Y. Yamamoto, Rev. Mod. Phys. **82**, 1489 (2010).
[4] S. O. Demokritov *et al.*, Nature **443**, 430 (2006).
[5] J. Klaers, J. Schmitt, F. Vewinger, M. Weitz, Nature **468**, 545 (2010).
[6] J. Fortágh, C. Zimmermann, Rev. Mod. Phys. **79**, 235 (2007).
[7] A. Sørensen, L.-M. Duan, J. I. Cirac, P. Zoller, Nature **409**, 63 (2000).
[8] I. Buluta, F. Nori, Science **326**, 108 (2009).
[9] M. Riedel *et al.*, Nature **464**, 1170 (2010).
[10] P. Böhi *et al.*, Nature Phys. **5**, 592 (2009).
[11] P. Treutlein *et al.*, Fortschr. Phys. **54**, 702 (2006).
[12] T. Hecht, Diploma Thesis, Technische Universität München Max-Planck-Institut für Quantenoptik (2004).
[13] D. Press, T. Ladd, B. Zhang, Y. Yamamoto, Nature **456**, 218 (2008).
[14] J. Berezovsky, M. H. Mikkelsen, N. G. Stoltz, L. A. Coldren, D. Awschalom, Science **320**, 349 (2008).
[15] D. Press *et al.* Nature Photonics **4**, 367 (2010).
[16] Y. Li, P. Treutlein, J. Reichel, A. Sinatra, Eur. Phys. J. B **68**, 365 (2009).
[17] E. Brion, K. Mølmer, M. Saffman, Phys. Rev. Lett. **99**, 260501 (2007).
[18] M. D. Lukin, M. Fleischhauer, R. Cote, L. M. Duan, D. Jaksch, J. I. Cirac, P. Zoller, Phys. Rev. Lett. **87**, 037901 (2001).
[19] P. Rabl *et al.* Phys. Rev. Lett. **97**, 033003 (2006).
[20] M. Nielsen, I. & Chuang, *Quantum computation and quantum information* (Cambridge University Press, 2000).
[21] S. Lloyd, Phys. Rev. Lett. **75**, 346 (1995).
[22] S. Braunstein and P. van Loock, Rev. Mod Phys. **77**, 513 (2005).
[23] J. Altepeter,D. James, P. Kwiat, Lect. Notes Phys. **649**, 113 (2004).
[24] T. Pellizzari, S. A. Gardiner, J. I. Cirac, P. Zoller, Phys. Rev. Lett. **75**, 3788 (1995).
[25] Y. Colombe *et al.*, Nature **450**, 272 (2007).
[26] K. Henschel, J. Majer, J. Schmiedmayer, H. Ritsch, Phys. Rev. A **82**, 033810 (2010).
[27] T. P. Purdy, D. M. Stamper-Kurn, Appl. Phys. B **90**, 401 (2008).
[28] S. B. Zheng and G. C. Guo, Phys. Rev. Lett. **85**, 2392 (2000).
[29] T. Ladd *et al.*, Nature **464**, 45 (2010).

Tim Byrnes Tim Byrnes completed his Ph.D. from the University of New South Wales in 2003. In 2004, he moved to Japan to commence a postdoctoral fellowship at the University of Tokyo and the National Institute of Informatics. He is currently assistant professor at the National Institute of Informatics. His current interests are in the fields of quantum simulation, quantum computation, and condensed matter physics.